

# Probabilistic Constellation Shaping With Denoising Diffusion Probabilistic Models: A Novel Approach

Mehdi Letafati, Samad Ali, and Matti Latva-aho

Centre for Wireless Communications, University of Oulu, Oulu, Finland  
{mehdi.letafati, samad.ali, matti.latva-aho}@oulu.fi

**Abstract**—With the incredible results achieved from generative pre-trained transformers (GPT) and diffusion models, generative AI (GenAI) is envisioned to yield remarkable breakthroughs in various industrial and academic domains. In this paper, we utilize denoising diffusion probabilistic models (DDPM), as one of the state-of-the-art generative models, for probabilistic constellation shaping in wireless communications. While the geometry of constellations is predetermined by the networking standards, probabilistic constellation shaping can help enhance the information rate and communication performance by designing the probability of occurrence (generation) of constellation symbols. Unlike conventional methods that deal with an optimization problem over the discrete distribution of constellations, we take a radically different approach. Exploiting the “denoise-and-generate” characteristic of DDPMs, the key idea is to learn how to generate constellation symbols out of noise, “mimicking” the way the receiver performs symbol reconstruction. By doing so, we make the constellation symbols sent by the transmitter, and what is inferred (reconstructed) at the receiver become as similar as possible. Our simulations show that the proposed scheme outperforms deep neural network (DNN)-based benchmark and uniform shaping, while providing *network resilience* as well as *robust out-of-distribution performance* under low-SNR regimes and non-Gaussian noise. Notably, a threefold improvement in terms of mutual information is achieved compared to DNN-based approach for 64-QAM geometry.

**Index Terms**—AI-native wireless, diffusion models, generative AI, network resilience, wireless AI.

## I. INTRODUCTION

The emergence of generative models has made a paradigm shift in the realm of artificial intelligence (AI) towards generative AI (GenAI)-based systems [1]. Innovative approaches in GenAI have attracted significant attention from both academia and industry, garnering extensive research and development efforts. In this regard, the evolution of diffusion models [2], as the state-of-the-art family of generative models, is considered as one of the key factors in the recent breakthroughs of GenAI. It has showcased remarkable results with famous solutions such as ImageGen by Google Brain and DALL.E 2 by OpenAI, to name a few. Through the lens of data communication and networking, “connected intelligence” is envisioned as the most significant driving force in the sixth generation (6G) of wireless communications [3]–[6]. It is envisioned that machine learning (ML) and AI algorithms are widely incorporated into wireless systems to realize “AI-native” systems. This highlights the need for novel AI solutions to be tailored for the emerging 6G scenarios.

### A. Literature Review

Although diffusion models have shown remarkable results in various applications within the computer science commu-

nity, such as natural language processing (NLP), computer vision, and medical imaging [7], there are *only a few papers in communication literature that have started looking into the applications of diffusion models for wireless systems* [8]–[11]. Notably, the incorporation of diffusion models into wireless communication problems is still in its infancy, and we hope that our paper sheds light on some of the possible directions.

The authors in [8] propose a workflow for wireless network management via utilizing diffusion models, highlighting their exploration capability for wireless network management. A preprint [9] employs diffusion models to improve the performance of receiver in terms of noise and channel estimation error removal. The authors employ an autoencoder (AE) in addition to their diffusion model. However, the output signals of the encoder does not necessarily follow the standard shape of constellation symbols, making the scheme inapplicable to real-world wireless systems. Moreover, implementing two different ML models, each with a distinct objective function can impose computational overhead to the network. Denoising diffusion probabilistic model (DDPM) is utilized in [10] to generate synthetic channel realizations for an AE-based end-to-end wireless system. The authors highlight the promising performance of diffusion models as an alternative to generative adversarial network (GAN)-based models. They show that GANs have unstable training and less diversity in generation performance, because of their “adversarial” training nature, while DDPMs maintain a more stable training process and a better generalization during inference. In [11], noise-conditioned score networks are employed for channel estimation in multi-input-multi-output (MIMO) wireless communications. RefineNet neural architecture is implemented to estimate the gradient of the log-prior of wireless channels. The results imply a competitive performance for in- and out-of-distribution (OOD) scenarios compared to GANs.

### B. Our Work

With the aid of GenAI, our general goal is to take a step towards an *AI-native* system [3]–[5], in which we can continuously design radio signals, adapt to changes, and realize “mutual understanding” between communication parties, instead of blindly transmitting information symbols. In this paper, we study the application of diffusion models, the state-of-the-art generative model in GenAI literature, for probabilistic constellation shaping in wireless communications. *To the best of our knowledge, this is the first paper that proposes diffusion models for constellation shaping in wireless communications.*

**Setting the Stage:** The choice of constellations can significantly affect the performance of communication systems. Recently, DNNs are proposed for geometric shaping [12]–[14]. They typically employ AEs and let the neural model learn constellation symbols for transmission. This results in arbitrary forms of constellation points that might not be compliant with wireless standards such as the 3rd Generation Partnership Project (3GPP) [15]. In such scenarios, probabilistic constellation shaping can help enhance the information rate and decoding performance of communication systems [12]. It designs the probability of occurrence (generation) of constellation symbols within the corresponding geometry.

**Our Contributions:** Unlike previous works that try to deal with the optimization of constellations over discrete distributions via iterative optimization methods or deep neural networks (DNN) [12], we offer a radically different approach—we exploit the “denoise-and-generate” characteristic of DDPMs for probabilistic shaping. First, a DDPM is trained with the aim of learning the diffusion process for generating constellation symbols out of noise. Within each transmission slot (TS), the transmitter runs the model to probabilistically shape (generate) the constellation symbols according to the signal-to-noise ratio (SNR) level. Intuitively, the goal is to do shaping in a way that the information-bearing constellation symbols generated at the transmitter, and what is inferred (reconstructed) at the receiver become as similar as possible, resulting in as few mismatches between the communication parties as possible. To fulfill this requirement, the transmitter exploits the “denoise-and-generate” characteristic of DDPMs, and “mimics” the way the receiver performs symbol reconstruction. (More details are provided in Section III.) We show that our proposed approach outperforms DNN-based scheme with trainable constellation layer and neural demapper [12]. Notably, we show a threefold improvement in terms of mutual information metric compared to DNN-based solution for 64-QAM geometry. Our results also highlight that the proposed DDPM-based scheme is *resilient* against low-SNR regimes. We also demonstrate a robust OOD performance under non-Gaussian noise, compared to other benchmarks.

In what follows, we first introduce DDPM framework in Section II. System model and the proposed scheme are introduced in Section III. Furthermore, the neural architecture and the proposed algorithms for probabilistic constellation shaping are addressed in this section. Numerical results are studied in Section IV, and Section V concludes the paper.<sup>1</sup>

<sup>1</sup>Vectors and matrices are represented, respectively, by bold lower-case and upper-case symbols.  $|\cdot|$  and  $\|\cdot\|$  respectively denote the absolute value of a scalar variable and the  $\ell_2$  norm of a vector. Notation  $\mathcal{N}(\mathbf{x}; \boldsymbol{\mu}, \boldsymbol{\Sigma})$  stands for the multivariate normal distribution with mean vector  $\boldsymbol{\mu}$  and covariance matrix  $\boldsymbol{\Sigma}$  for a random vector  $\mathbf{x}$ . Similarly, complex normal distribution with the corresponding mean vector and covariance matrix is denoted by  $\mathcal{CN}(\boldsymbol{\mu}, \boldsymbol{\Sigma})$ . Moreover, the expected value of a random variable (RV) is denoted by  $\mathbb{E}[\cdot]$ . Sets are denoted by calligraphic symbols.  $\mathbf{0}$  and  $\mathbf{I}$  respectively show all-zero vector and identity matrix of the corresponding size. Moreover,  $[N]$ , (with  $N$  as integer) denotes the set of all integer values from 1 to  $N$ , and  $\text{Unif}[N]$  (for  $N > 1$ ) denotes discrete uniform distribution with samples between 1 to  $N$ . Also,  $\delta(\cdot)$  denotes the Dirac function.

## II. PRELIMINARIES ON DDPMs

Diffusion models are a new class of state-of-the-art probabilistic generative models inspired by non-equilibrium thermodynamics [2]. Let  $\mathbf{x}_0$  be a data sample from some distribution  $q(\mathbf{x}_0)$ . For a finite number  $T$  of time-steps, the forward diffusion process  $q(\mathbf{x}_t|\mathbf{x}_{t-1})$  is defined by adding Gaussian noise according to a “variance schedule”  $0 < \beta_1 < \beta_2 < \dots < \beta_T < 1$  at each time-step  $t \in [T]$ . This is,

$$q(\mathbf{x}_t|\mathbf{x}_{t-1}) \sim \mathcal{N}(\mathbf{x}_t; \sqrt{1 - \beta_t}\mathbf{x}_{t-1}, \beta_t\mathbf{I}), \quad (1)$$

$$q(\mathbf{x}_{1:T}|\mathbf{x}_0) = \prod_{t=1}^T q(\mathbf{x}_t|\mathbf{x}_{t-1}). \quad (2)$$

Invoking (2), the data sample gradually loses its distinguishable features as the time-step goes on, where with  $T \rightarrow \infty$ ,  $\mathbf{x}_T$  approaches an isotropic Gaussian distribution with covariance matrix  $\boldsymbol{\Sigma} = \sigma^2\mathbf{I}$  for some  $\sigma > 0$  [2]. According to (1), each new sample at time-step  $t$  can be drawn from a conditional Gaussian distribution with mean vector  $\mu_t = \sqrt{1 - \beta_t}\mathbf{x}_{t-1}$  and covariance matrix  $\boldsymbol{\Sigma}_t^2 = \beta_t\mathbf{I}$ . Hence, the forward process is realized by sampling from a Gaussian noise  $\boldsymbol{\epsilon}_{t-1} \sim \mathcal{N}(\mathbf{0}, \mathbf{I})$  and setting

$$\mathbf{x}_t = \sqrt{1 - \beta_t}\mathbf{x}_{t-1} + \sqrt{\beta_t}\boldsymbol{\epsilon}_{t-1}. \quad (3)$$

A useful property for the forward process in (3) is that we can sample  $\mathbf{x}_t$  at any arbitrary time step  $t$ , via recursively applying the reparameterization trick from ML literature [16]. This results in the following formulation.

$$\mathbf{x}_t = \sqrt{\bar{\alpha}_t}\mathbf{x}_0 + \sqrt{1 - \bar{\alpha}_t}\boldsymbol{\epsilon}_0, \quad (4)$$

$$q(\mathbf{x}_t|\mathbf{x}_0) \sim \mathcal{N}(\mathbf{x}_t; \sqrt{\bar{\alpha}_t}\mathbf{x}_0, (1 - \bar{\alpha}_t)\mathbf{I}), \quad (5)$$

where  $\bar{\alpha}_t = \prod_{i=1}^t (1 - \alpha_i)$  and  $\alpha_t = 1 - \beta_t$ .

Now the problem is to reverse the process in (4) and sample from  $q(\mathbf{x}_{t-1}|\mathbf{x}_t)$ , so that we regenerate the true samples from some Gaussian noise  $\mathbf{x}_T$ . According to [2], for  $\beta_t$  small enough,  $q(\mathbf{x}_{t-1}|\mathbf{x}_t), \forall t \in [T]$  also follows Gaussian distribution. However, we cannot easily estimate the distribution, since it requires knowing the distribution of all possible data samples. Hence, to approximate the conditional probabilities and run the reverse diffusion process, we need to learn a probabilistic model  $p_{\boldsymbol{\theta}}(\mathbf{x}_{t-1}|\mathbf{x}_t)$ , parameterized by  $\boldsymbol{\theta}$ . Accordingly, we can write

$$p_{\boldsymbol{\theta}}(\mathbf{x}_{t-1}|\mathbf{x}_t) \sim \mathcal{N}(\mathbf{x}_{t-1}; \boldsymbol{\mu}_{\boldsymbol{\theta}}(\mathbf{x}_t, t), \boldsymbol{\Sigma}_{\boldsymbol{\theta}}(\mathbf{x}_t, t)), \quad (6)$$

$$p_{\boldsymbol{\theta}}(\mathbf{x}_{0:T}) = p(\mathbf{x}_T) \prod_{t=1}^T p_{\boldsymbol{\theta}}(\mathbf{x}_{t-1}|\mathbf{x}_t). \quad (7)$$

Now the problem simplifies to learning the mean vector  $\boldsymbol{\mu}_{\boldsymbol{\theta}}(\mathbf{x}_t, t)$  and the covariance matrix  $\boldsymbol{\Sigma}_{\boldsymbol{\theta}}(\mathbf{x}_t, t)$  for the probabilistic model  $p_{\boldsymbol{\theta}}(\cdot)$ , where a neural network (NN), with parameter  $\boldsymbol{\theta}$ , can be trained to approximate (learn) the reverse process. We note that if we condition the reverse process on  $\mathbf{x}_0$ , this conditional probability becomes tractable [2]. Hence, when we have  $\mathbf{x}_0$  as a reference, we can take a small step

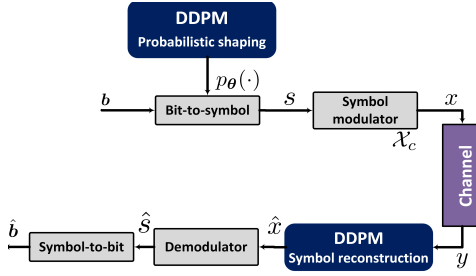


Fig. 1: System model overview.

backwards to generate data samples, and the reverse step is formulated as  $q(\mathbf{x}_{t-1}|\mathbf{x}_t, \mathbf{x}_0)$ . Mathematically, we have

$$q(\mathbf{x}_{t-1}|\mathbf{x}_t, \mathbf{x}_0) \sim \mathcal{N}(\mathbf{x}_{t-1}; \tilde{\boldsymbol{\mu}}(\mathbf{x}_t, \mathbf{x}_0, t), \tilde{\boldsymbol{\beta}}_t \mathbf{I}), \quad (8)$$

which is obtained by utilizing Bayes rule, where

$$\tilde{\boldsymbol{\mu}}(\mathbf{x}_t, \mathbf{x}_0, t) = \frac{\sqrt{\bar{\alpha}_t}(1 - \bar{\alpha}_{t-1})}{1 - \bar{\alpha}_t} \mathbf{x}_t + \frac{\sqrt{\bar{\alpha}_{t-1}}\beta_t}{1 - \bar{\alpha}_t} \mathbf{x}_0, \quad (9)$$

$$\tilde{\boldsymbol{\beta}}_t = \frac{1 - \bar{\alpha}_{t-1}}{1 - \bar{\alpha}_t} \beta_t. \quad (10)$$

Invoking (10), one can infer that the covariance matrix in (8) has no learnable parameter. Hence, we simply need to learn the mean vector  $\tilde{\boldsymbol{\mu}}(\mathbf{x}_t, \mathbf{x}_0, t)$ . To further simplify (9), we note that thanks to the reparameterization trick and with a similar approach to (4), we can express  $\mathbf{x}_0$  as follows.

$$\mathbf{x}_0 = \frac{1}{\sqrt{\bar{\alpha}_t}} (\mathbf{x}_t - \sqrt{1 - \bar{\alpha}_t} \boldsymbol{\epsilon}_t). \quad (11)$$

Substituting  $\mathbf{x}_0$  in (9) by (11) results in

$$\tilde{\boldsymbol{\mu}}(\mathbf{x}_t, \mathbf{x}_0, t) = \frac{1}{\sqrt{\bar{\alpha}_t}} \left( \mathbf{x}_t - \frac{1 - \alpha_t}{\sqrt{1 - \bar{\alpha}_t}} \boldsymbol{\epsilon}_t \right). \quad (12)$$

Now we can learn the conditioned probability distribution  $p_\theta(\mathbf{x}_{t-1}|\mathbf{x}_t)$  by training a NN that approximates  $\tilde{\boldsymbol{\mu}}(\mathbf{x}_t, \mathbf{x}_0, t)$ . Therefore, we simply need to set the approximated mean vector  $\boldsymbol{\mu}_\theta(\mathbf{x}_t, t)$  to have the same form as the target mean vector  $\tilde{\boldsymbol{\mu}}(\mathbf{x}_t, \mathbf{x}_0, t)$ . Since  $\mathbf{x}_t$  is available at time-step  $t$ , we can reparameterize the NN to make it approximate  $\boldsymbol{\epsilon}_t$  from the input  $\mathbf{x}_t$ . Compiling these facts results in

$$\boldsymbol{\mu}_\theta(\mathbf{x}_t, t) = \frac{1}{\sqrt{\bar{\alpha}_t}} \left( \mathbf{x}_t - \frac{1 - \alpha_t}{\sqrt{1 - \bar{\alpha}_t}} \boldsymbol{\epsilon}_\theta(\mathbf{x}_t, t) \right), \quad (13)$$

where  $\boldsymbol{\epsilon}_\theta(\mathbf{x}_t, t)$  denotes our NN. We can now define the loss function  $\mathcal{L}_t$  for time-step  $t \in [T]$ , aiming to minimize the difference between  $\boldsymbol{\mu}_\theta(\mathbf{x}_t, t)$  and  $\tilde{\boldsymbol{\mu}}(\mathbf{x}_t, \mathbf{x}_0, t)$ .

$$\begin{aligned} \mathcal{L}_t &= \mathbb{E}_{\substack{t \sim \text{Unif}[T] \\ \mathbf{x}_0 \sim q(\mathbf{x}_0) \\ \boldsymbol{\epsilon}_0 \sim \mathcal{N}(\mathbf{0}, \mathbf{I})}} \left[ \|\boldsymbol{\epsilon}_t - \boldsymbol{\epsilon}_\theta(\mathbf{x}_t, t)\|^2 \right] \\ &= \mathbb{E}_{\substack{t \sim \text{Unif}[T] \\ \mathbf{x}_0 \sim q(\mathbf{x}_0) \\ \boldsymbol{\epsilon}_0 \sim \mathcal{N}(\mathbf{0}, \mathbf{I})}} \left[ \|\boldsymbol{\epsilon}_t - \boldsymbol{\epsilon}_\theta(\sqrt{\bar{\alpha}_t} \mathbf{x}_0 + \sqrt{1 - \bar{\alpha}_t} \boldsymbol{\epsilon}_t, t)\|^2 \right]. \end{aligned} \quad (14)$$

Invoking (14), at each time-step  $t$ , the DDPM model takes  $\mathbf{x}_t$  as input and returns the distortion components  $\boldsymbol{\epsilon}_\theta(\mathbf{x}_t, t)$ . Also,  $\boldsymbol{\epsilon}_t$  denotes the diffused noise term at time step  $t$ ,

### III. SYSTEM MODEL AND PROPOSED SCHEME

Fig. 1 demonstrates the communication system under consideration. The system takes the information bitstream and maps it onto hypersymbols  $s \in \mathcal{S}$ ,  $\mathcal{S} = \{1, \dots, M\}$ , according to the learnable distribution  $p_\theta(s)$  (parameterized by  $\theta$ ), where  $M$  denotes the modulation order. In this paper,  $\theta$  is realized by a DDPM, which is trained and shared with the transmitter and receiver. The sequence of hypersymbols is then fed into a symbol modulator which maps each symbol  $s$  into a constellation point  $x \in \mathcal{X}_c$ , with  $\mathcal{X}_c$  showing the set of constellation points. Each symbol is generated according to the distribution  $p_\theta(s)$ . In other words, the frequency of sending a bitstream over the constellation point  $x = g(s)$  corresponds to the parametric distribution  $p_\theta(s)$ , where  $g$  denotes the modulation functionality. Accordingly, we have

$$p_\theta(x) = \sum_{s \in \mathcal{S}} \delta(x - g(s)) p_\theta(s), \quad \forall x \in \mathcal{X}_c. \quad (15)$$

As motivated in Section I, our focus in this work is on probabilistic shaping, and hence, constellation geometry is determined in advance according to network configurations. Thus, the design of modulator function  $g(\cdot)$  is not of interest in this work, and we adhere to standard constellation schemes, such as QAM, in order to propose a system which is compliant with the real-world communication systems. In addition, similar to [12], we also assume that the bits-to-symbols mapper is known. Hence, we have a one-to-one mapping between the constellation point  $x$  and the information symbol  $s$ , and the transmitter's output is directly sampled from  $p_\theta(\cdot)$ . Information-bearing signal  $x$  is then sent over the communication channel, and the channel output  $y$  is observed at the receiver. Then the receiver needs to reconstruct the transmitted symbols by approximating the posterior distribution  $p(s|y)$  given the channel output. To do so, the receiver leverages the trained DDPM and maps each received sample  $y$  to a probability distribution over the set of symbols  $\mathcal{S}$ . Having this approximation, symbols can be obtained at the receiver's de-modulator, and the information bits can be reconstructed using the prevalent symbol-to-bit mappers.

#### A. Proposed Approach

**Setting the Stage:** Intuitively speaking, the goal is to probabilistically shape the constellation symbols by finding a proper  $p_\theta(\cdot)$ , such that the information-bearing symbols sent by the transmitter, and what is inferred at the receiver become as similar as possible,<sup>2</sup> resulting in as few mismatches between the communication parties as possible. This fact, together with the characteristic of diffusion models to “denoise-and-generate”, motivates us to propose the following DDPM-based approach for probabilistic constellation shaping. The key idea to fulfill the desired similarity is that the transmitter “mimics” the way the receiver would perform the reconstruction of symbols. Hence, the transmitter probabilistically

<sup>2</sup>This “similarity” will be quantitatively evaluated in Section IV using the widely-adopted mutual information metric.

generates the constellations in a way that would be similar to the process of denoising and reconstruction (regeneration) at the receiver. This also helps facilitate having “mutual understanding” of how to map and de-map the information symbols over time, realizing kind of *native intelligence* among communication parties. Motivated by these facts, our step-by-step solution can be elaborated on as follows.

1) *DDPM Training*: A DDPM is trained based on the loss function given in (14). This corresponds to training the parameter  $\theta$  for our probabilistic shaping scheme in (15). The goal is to train a diffusion process to generate constellation symbols (with the pre-determined geometry) out of noise. The process is summarized in Algorithm 1, which is inspired by the seminal paper of DDPM by Ho *et. al*, 2020 [2]. Training can be carried out in a central cloud, or an edge server and then downloaded by the communication entities. The trained model is deployed at the transmitter and the receiver.

2) *Link quality estimation using channel SNR*: Within each TS, the transmitter first estimates the quality of communication link. This can be carried out using the pilot signals sent by the destination node, at the beginning of each TS, and the SNR level of communication channel can be calculated [18].

3) *Probabilistic shaping*: The trained DDPM is run at the transmitter to probabilistically shape (generate) the constellation symbols according to the channel SNR. To do so, the transmitter first takes  $N_s$  samples from the set of constellation symbols  $\mathcal{X}_c$  uniformly at random.<sup>3</sup> The goal is not to uniformly map information symbols to constellation points. Rather, we aim to generate the constellation symbols in a way that the information-bearing constellation symbols sent by the transmitter, and what is inferred (reconstructed) at the receiver become as similar as possible. For instance, when the communication channel is experiencing high levels of noise, i.e., in low-SNR regime, we intuitively expect that most often, the receiver would be able to decode the symbols corresponding to the points that are relatively far from each other in the constellation geometry, while the other points are prone to being decoded incorrectly. Thus, the transmitter wishes to probabilistically reshape the constellation symbols in a way that would be straightforward to denoise and reconstruct (regenerate) at the receiver. To do so, the transmitter samples  $N_s$  random noise with average power  $\delta^2$ , and injects them to the uniformly-sampled symbols. The power of synthetic noise,  $\delta^2$ , is calculated according to the channel SNR,  $\Gamma$ , which is obtained at Step 2, and can be formulated as  $\delta^2 = P10^{\Gamma/10}$ , where  $P$  denotes the average transmit power. The noisy version of samples is then fed into the trained DDPM, and the reverse diffusion process is run to denoise and generate symbols out of the synthetically-noisy samples. In other words, the transmitter tries to mimic the way the receiver performs the reconstruction (regeneration) of symbols, when it receives noisy symbols. The distribution of the generated samples at the output of the DDPM block

<sup>3</sup>The sample size  $N_s$  can be regarded as the number of observations to form (generate) the empirical distribution of our probabilistic shaping.

---

#### Algorithm 1 Training algorithm of DDPM

---

**Hyper-parameters:** Number of time-steps  $T$ , neural architecture  $\epsilon_\theta(\cdot, t)$ , variance schedule  $\beta_t$ , and  $\bar{\alpha}_t, \forall t \in [T]$ .

**Input:** Training samples from the constellation geometry  $\mathcal{X}_c$ .

**Output:** Trained neural model for DDPM.

```

1: while the stopping criteria are not met do
2:   Randomly sample  $\mathbf{x}_0$  from  $\mathcal{X}_c$ 
3:   Randomly sample  $t$  from  $\text{Unif}[T]$ 
4:   Randomly sample  $\epsilon$  from  $\mathcal{N}(\mathbf{0}, \mathbf{I})$ 
5:   Take gradient descent step on
6:      $\nabla_\theta \|\epsilon - \epsilon_\theta(\sqrt{\bar{\alpha}_t}\mathbf{x}_0 + \sqrt{1 - \bar{\alpha}_t}\epsilon, t)\|^2$ 
7: end while

```

---

#### Algorithm 2 DDPM sampling: Probabilistic shaping at transmitter

---

**Hyper-parameters:** Number of time-steps  $T$ , trained neural model  $\theta$ , constellation geometry  $\mathcal{X}_c$

**Input:** Channel SNR  $\Gamma$ .

```

1: Randomly sample  $\tilde{\mathbf{x}}_s$ , with size  $N_s$ , from set  $\mathcal{X}_c$ 
2: Randomly sample  $\tilde{\mathbf{n}}$ , with size  $N_s$ , from  $\mathcal{N}(\mathbf{0}, \mathbf{I})$ 
3:  $\tilde{\mathbf{y}}_r = \tilde{\mathbf{x}}_s + \delta\tilde{\mathbf{n}}$ 
4:  $\mathbf{x}_T = \tilde{\mathbf{y}}_r$ 
5: for  $t = T, \dots, 1$  do
6:    $\mathbf{z} \sim \mathcal{N}(\mathbf{0}, \mathbf{I})$  if  $t > 1$ , else  $\mathbf{z} = \mathbf{0}$ 
7:    $\mathbf{x}_{t-1} = \frac{1}{\sqrt{\alpha_t}} \left( \mathbf{x}_t - \frac{1 - \alpha_t}{\sqrt{1 - \alpha_t}} \epsilon_\theta(\mathbf{x}_t, t) \right) + \sqrt{1 - \alpha_t} \mathbf{z}$ 
8: end for
9:  $\psi = \text{proj}_{\mathcal{X}_c}(\mathbf{x}_0)$ 
10:  $\mathbf{c} = \text{count}(\psi, \mathcal{X}_c)$ 
11: return  $p_\theta = \mathbf{c}/N_s$ 

```

---

is considered as the output probabilistic constellations onto which the information symbols are mapped to be sent.

The overall algorithm is proposed in Algorithm 2, where the main loop corresponds to the reverse diffusion process from time-step  $T$  to 1, according to 13. Also,  $\text{proj}_{\mathcal{S}}(\mathbf{x})$  stands for the projection operator, which maps the elements of vector  $\mathbf{x}$  onto the nearest elements in the set  $\mathcal{S}$ . Moreover,  $\text{count}(\mathbf{x}, \mathcal{S})$  outputs a vector with size  $|\mathcal{S}|$ , with elements representing the number of occurrences of the elements of set  $\mathcal{S}$  in vector  $\mathbf{x}$ . Notably,  $\psi$  in Algorithm 2 denotes the probabilistically-shaped constellation points at the output of the transmitter’s DDPM block, and  $p_\theta$  stands for the corresponding distribution inferred by the diffusion model.

4) *Symbol reconstruction at the receiver*: After generating constellation symbols, information signals are sent according to the probabilistic constellations. The symbols are received by the receiver. Then the receiver runs the diffusion model to reconstruct (regenerate) the symbols from the received noisy signals. The corresponding algorithm for this step is proposed in Algorithm 3. Starting from the received batch of noisy symbols, denoted by  $\mathbf{y}_r$ , for each time step  $t \in \{T, T-1, \dots, 1\}$ , the NN outputs  $\epsilon_\theta(\hat{\mathbf{x}}_t, t)$  to approximate the residual noise within the batch of symbols, and the sampling algorithm is run according to Line 4 of the algorithm, in order to sample  $\hat{\mathbf{x}}_{t-1}$ . The process is executed for  $T$  steps.<sup>4</sup>

<sup>4</sup>We emphasize that within each TS, while the channel coherence time is respected, the channel SNR remains unchanged compared to the one that is utilized by the transmitter for the constellation shaping.

---

**Algorithm 3** DDPM sampling: Symbol reconstruction at receiver

---

**Hyper-parameters:** Number of time-steps  $T$ , trained neural model  $\theta$ , constellation geometry  $\mathcal{X}_c$

**Input:** Received signal  $y_r$

- 1:  $\hat{\mathbf{x}}_T = y_r$
  - 2: **for**  $t = T, \dots, 1$  **do**
  - 3:  $\mathbf{z} \sim \mathcal{N}(\mathbf{0}, \mathbf{I})$  if  $t > 1$ , else  $\mathbf{z} = \mathbf{0}$
  - 4:  $\hat{\mathbf{x}}_{t-1} = \frac{1}{\sqrt{\alpha_t}} \left( \hat{\mathbf{x}}_t - \frac{1-\alpha_t}{\sqrt{1-\alpha_t}} \epsilon_\theta(\hat{\mathbf{x}}_t, t) \right) + \sqrt{1-\alpha_t} \mathbf{z}$
  - 5: **end for**
  - 6: **return**  $\text{proj}_{\mathcal{X}_c}(\hat{\mathbf{x}}_0)$
- 

#### IV. EVALUATIONS

In this section, we carry out numerical evaluations, in order to highlight the performance of the proposed scheme compared to other benchmarks. Specifically, we show that our DDPM-based approach achieves a threefold improvement in terms of mutual information compared to DNN-based solution for 64-QAM geometry. We also show that the proposed DDPM can provide *native resilience* for the communication system under low-SNR regimes and non-Gaussian noise.

We employ a NN comprised of 3 hidden linear layers each of which has 128 neurons with softplus activation functions. The output layer is a simple linear layer with the same shape as input. Inspired by the Transformer paper [17], we share the parameters of the NN across time-steps via multiplying the embeddings of time-step and incorporating them into the model. For training the diffusion model, we use adaptive moment estimation (Adam) optimizer with learning rate  $\lambda = 10^{-3}$ . We consider QAM geometry as a widely-adopted constellation format in wireless networks [4], [6], [12]. Moreover, we set  $T = 100$ , and the stopping criterion in Algorithm 1 is met when reaching the maximum number of epochs [9]–[11], which is set to 1000 epochs.

Fig. 2, demonstrates data visualization for sampling phase, corresponding to Algorithms 2 and 3. The first row corresponds to the constellation generation steps that are performed at the transmitter (Algorithm 2), and the second row corresponds to the reconstruction at the receiver (Algorithm 3). This is repeated for different SNRs to visualize the constellation shaping performance of our DDPM under different levels of noise. Comparing the output of our probabilistic constellation generation algorithm (the first row) and the reconstructed symbols at the receiver (the second row), we can observe that the idea of synthetically mimicking the functionality of receiver for shaping the constellation symbols (addressed in Section III-A) has helped the transmitter generate symbols that are quite similar to the ones that are actually reconstructed by the receiver. This can improve the communication performance by decreasing the mismatch between the way the transmitter decides to convey the information, and the way the receiver decodes the symbols. This “similarity” is quantitatively measured in terms of mutual information in the next figure. According to the figure, when the communication system is experiencing low-SNR regimes, the probabilistic model demonstrates a non-uniform distribution over constellation points, with higher probabilities

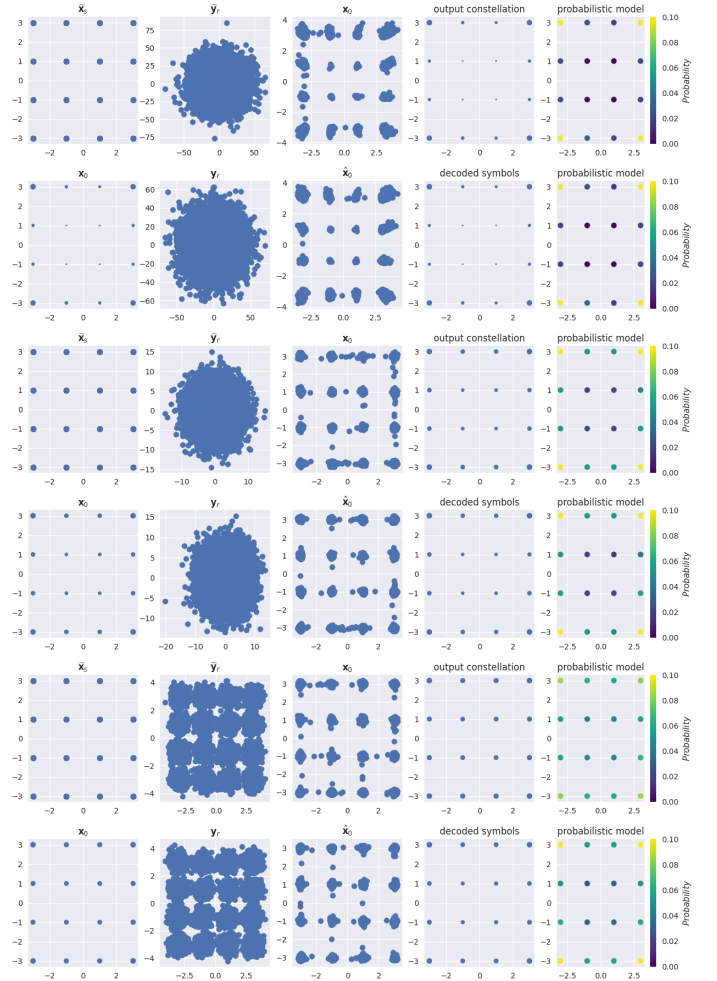


Fig. 2: Generation process at the transmitter, and the reconstruction at receiver for SNR values set to  $-25$ ,  $-10$ , and  $10$  dB, respectively.

assigned to the points that are at the furthest distance from each other in the constellation geometry. This is aligned with what we intuitively expect from a communication system under low-SNR regimes to frequently map information bits to constellation symbols that are far apart from each other. Increasing the SNR, the probabilistic shaping tends to uniform distribution, which is also aligned with one’s intuition about communication systems.

Fig. 3 demonstrates the mutual information between the probabilistically-generated symbols at the output of transmitter (i.e., the channel input), and the reconstructed ones at the receiver. The mutual information metric can be interpreted as the quantitative measure to study the “mutual similarity” among communication parties as discussed in Section III-A. For this experiment, we consider both cases of additive white Gaussian noise (AWGN) channel and also non-Gaussian noise to show the OOD performance of our scheme. For the benchmark, we consider a DNN model with trainable constellation layer and neural demapper as proposed in [12]. The DNN benchmark has three linear layers with 64 neurons at hidden layers and rectified linear unit (ReLU) activation



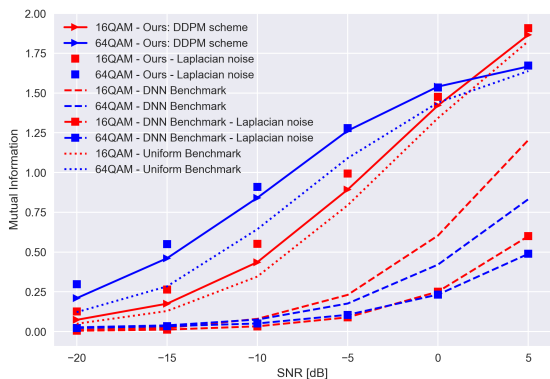


Fig. 3: Mutual information between the generated symbols at transmitter and the reconstructed ones at the receiver.

functions, and we considered 5000 training iterations with Adam optimizer. Fig. 3 clearly highlights the performance of our DDPM-based model in low-SNR regimes. Notably, although the DNN benchmark does not show any noticeable performance in SNR ranges below  $-5$  dB, even for the more straightforward scenario of 16-QAM (which is supposed to be less prone to errors and mismatches than 64-QAM case), our scheme achieves mutual information of around 1.25 bits for 64-QAM geometry, and 1 bit for 16-QAM geometry, respectively. Moreover, our scheme shows a threefold improvement compared to DNN-based benchmark for 64-QAM geometry and 0 dB SNR. These results clearly highlight that our main goal in realizing the “mutual understanding” among communication parties has been successfully achieved, and thanks to this understanding, the system is resilient under low-SNRs. To show the robustness of our scheme in OOD performance, we study the scenario of communication channels with non-Gaussian noise. We consider additive Laplacian noise with the same variance as that of AWGN scenario as our benchmark [6]. Remarkably, although we do not re-train our diffusion model with Laplacian noise, the performance of our DDPM-based approach does not change (even becomes better) under this non-Gaussian assumption (which is not seen during training), and the resultant mutual information curves follow the case of in-distribution scenario. However, the DNN benchmark experiences performance degradation under non-Gaussian assumption, although we also re-trained it with Laplacian noise. In Fig. 3, we also study another benchmark, which is uniform shaping. We examine this benchmark by disabling the DDPM block at the transmitter. We can see from the figure that still, the employed DDPM at receiver can outperform conventional DNN benchmark. Notably, the figure implies that our probabilistic shaping model with DDPMs employed at both the transmitter and the receiver outperforms the naive scheme of uniform shaping. This gap also increases when considering higher modulation orders, as it becomes more important to realize somewhat mutual understanding and smartly shaping the higher order constellation symbols.

## V. CONCLUSIONS

In this paper, we studied the application of DDPMs in probabilistic constellation shaping for wireless communica-

tions. We exploited the “denoise-and-generate” characteristic of DDPMs. The transmitter runs the model to probabilistically shape (generate) the constellation symbols and the receiver regenerates (reconstructs) the symbols from the received noisy signals. The key idea was that the transmitter mimics the way the receiver would do to reconstruct (regenerate) the symbols out of noisy signals, realizing “mutual understanding” to reduce the mismatch among communication parties. Our results highlighted the performance of our scheme compared to DNN-based demapper, while providing *network resilience* under low-SNR regimes and non-Gaussian noise.

## REFERENCES

- [1] P. Popovski. (2023, Jun. 11). “Communication engineering in the era of generative AI,” *Medium*, [Online]. Available: <https://petarpopovski-51271.medium.com/communication-engineering-in-the-era-of-generative-ai-703f44211933>
- [2] J. Ho, A. Jain, and P. Abbeel, “Denoising diffusion probabilistic models,” *Advances in Neural Information Processing Systems*, vol. 33, pp. 6840–6851, 2020.
- [3] 3GPP Release 18, “Study on Artificial Intelligence (AI)/Machine Learning (ML) for NR Air Interface RAN,” Meeting #112, Athens, Greece, Tech. Rep., 27th February – 3rd March 2023.
- [4] M. Merluzzi et al., “The Hexa-X project vision on artificial intelligence and machine learning-driven communication and computation co-design for 6G,” *IEEE Access*, vol. 11, pp. 65620–65648, Jun. 2023.
- [5] F. A. Aoudia, J. Hoydis, A. Valcarce, and H. Viswanathan, “Toward a 6G AI-native air interface,” *Nokia Bell Labs*, Mar. 2021. [Online]. Available: <https://onestore.nokia.com/asset/210299>.
- [6] M. Chafii, L. Bariah, S. Muhaidat, and M. Debbah, “Twelve scientific challenges for 6G: Rethinking the foundations of communications theory,” *IEEE Communications Surveys & Tutorials*, vol. 25, no. 2, pp. 868–904, Second quarter 2023.
- [7] B. Levac, A. Jalal, K. Ramchandran, and J. I. Tamir, “MRI reconstruction with side information using diffusion models,” *arXiv:2303.14795*, Jun. 2023. [Online]. Available: <https://arxiv.org/abs/2303.14795>.
- [8] Y. Liu, H. Du, D. Niyato, J. Kang, Z. Xiong, D. I. Kim, A. Jamalipour, “Deep generative model and its applications in efficient wireless network management: A tutorial and case study,” *arXiv preprint arXiv: 2303.17114*, Mar. 2023.
- [9] T. Wu, Z. Chen, D. He, L. Qian, Y. Xu, M. Tao, W. Zhang, “CDDM: Channel denoising diffusion models for wireless communications,” *arXiv preprint arXiv: 2305.09161*, May 2023.
- [10] M. Kim, R. Fritschek, and R. F. Schaefer, “Learning end-to-end channel coding with diffusion models,” *26th International ITG Workshop on Smart Antennas and 13th Conference on Systems, Communications, and Coding (WSA & SCC 2023)*, Braunschweig, Germany, Feb. 27 – Mar. 3, 2023, pp. 1–6.
- [11] M. Arvinte and J. I. Tamir, “MIMO channel estimation using score-based generative models,” *IEEE Trans. Wireless Commun.*, vol. 22, no. 6, pp. 3698–3713, Jun. 2023.
- [12] M. Stark, F. A. Aoudia, and J. Hoydis, “Joint learning of geometric and probabilistic constellation shaping,” *2019 IEEE Globecom Workshops (GC Wkshps)*, Waikoloa, HI, USA, 2019, pp. 1–6.
- [13] D. Korpi, M. Honkala, J. M. J. Huttunen, F. Aoudia, and J. Hoydis, “Waveform learning for reduced out-of-band emissions under a nonlinear power amplifier,” *arXiv preprint arXiv: 2201.05524*, Jan. 2022.
- [14] F. A. Aoudia and J. Hoydis, “Waveform learning for next-generation wireless communication systems,” *IEEE Transactions on Communications*, vol. 70, no. 6, pp. 3804–3817, Jun. 2022.
- [15] [Release 16] 3GPP. “Physical channels and modulation.” TS 38.211 (V16.2.0), July 2020.
- [16] D. P. Kingma, T. Salimans, and M. Welling “Variational dropout and the local reparameterization trick,” *Advances in Neural Information Processing Systems (NIPS 2015)*, vol. 28, 2015.
- [17] A. Vaswani, et al., “Attention is all you need,” *arXiv:1706.03762v7*, Aug. 2023. [Online]. Available: <https://arxiv.org/abs/1706.03762>.
- [18] X. Chen, D. W. K. Ng, W. Yu, E. G. Larsson, N. Al-Dhahir, and R. Schober, “Massive access for 5G and beyond,” *IEEE J. Sel. Areas Commun.*, vol. 39, no. 3, pp. 615–637, Mar. 2021.